

C₃-symmetric twisted organic salt as efficient mechano-/thermo-responsive molecule: a reusable, and sensitive, fluorescent thermometer

Banchhanidhi Prusti,^a Pralok K. Samanta,^b Niall J. English^c and Manab Chakravarty*^a

^aDepartment of Chemistry, Birla Institute of Science and Technology (BITS), Hyderabad Campus, Jawahar Nagar, Shameerpet Mandal, Hyderabad 500078, India

^bDepartment of Chemistry, School of Science, Gandhi Institute of Technology and Management (GITAM), Hyderabad 502329, India

^cSchool of Chemical and Bioprocess Engineering, University College Dublin, Dublin 4, Ireland

Contents:

1. Experimental section-----	S2
2. Synthetic scheme and characterization for C3PTZ -----	S2-S3
3. ¹ H, ¹³ C NMR spectra and HR-MS spectrum for C3PTZ -----	S3-S4
4. Methods and measurements-----	S4-S6
5. TGA plot, absorption and FL spectra for C3PTZ -----	S6
6. Frontier Molecular Orbitals (FMOs) and Natural transition orbitals (NTOs)-----	S7
7. Experimental absorption wavelength calculation table for C3PTZ -----	S8
8. Solvent dependent abs./FL spectra and conc. dependent abs./FL spectra-----	S8-S9
9. Solid-state absorption spectra with pressure and heat stimuli-----	S9
10. Temperature dependent FL spectra in solution-state-----	S9
11. Reversible thermochromic picture for C3PTZ -----	S10
12. Photophysical parameters table for C3PTZ -----	S10
13. Lifetime decay plot before and after pressure and heat stimuli-----	S11
14. Lifetime decay table for C3PTZ -----	S11
15. PXRD pattern for pristine, heated and fumed for C3PTZ -----	S12
16. Optimized structure for C3PTZ and their interplanar angles-----	S12
17. Non-covalent interaction (NCP) calculation and plot-----	S13
18. References-----	S13-S14

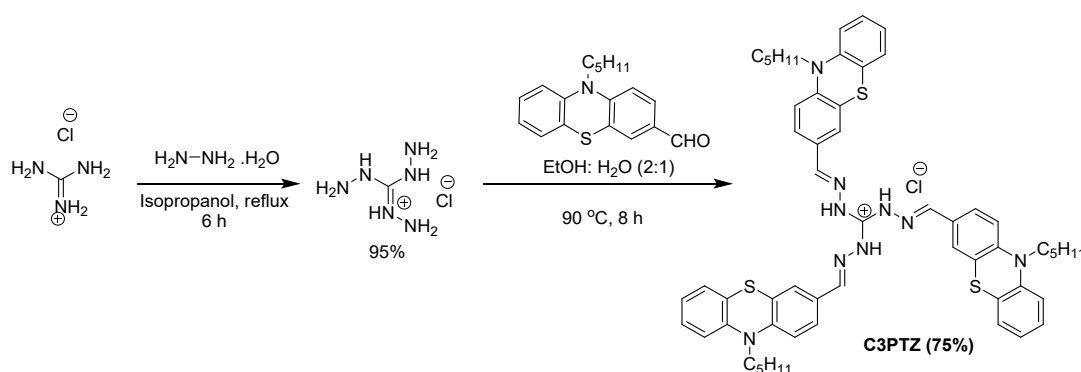
Experimental section

Materials: Phenothiazine, hydrazine hydrate and guanidinium chloride were purchased from Alfa aesar. All other reagents were purchased from common suppliers and used without further purification. Column chromatography was performed using Silica gel 100-200 mesh. Reactions were monitored by thin-layer chromatography on precoated silica gel 60 F254 plates (Merck & Co.) and were visualized by UV (mainly 365 nm). The ^1H and ^{13}C NMR spectra were recorded in CDCl_3 solution using Bruker Advance DRX (400 MHz). The signals were referenced to TMS, and the solvent used was deuterated chloroform (7.26 ppm in ^1H NMR, 77.16 ppm in ^{13}C NMR). Chemical shifts are reported in ppm, and multiplicities are indicated by s (singlet), d (doublet), t (triplet), and dd (doublet of a doublet). All data were plotted using Origin Pro 8.5 software.

Synthesis: C3PTZ was synthesized in a two-step manner. Initially, triamino guanidinium chloride (TAG) was obtained from guanidinium chloride (GC) in the following reported method.¹

Guanidinium chloride (1 mmol) was taken in 30 mL of isopropanol in a 100 mL round bottom flask. Hydrazine hydrate (50-60%) (4.5 mmol) was added to the above solution and was refluxed for 6 h. After the reaction, the precipitate was filtered and was washed with 50 mL of isopropanol to obtain TAG (yield: 95%).

TAG (1.10 g, 7.81 mmol) was dissolved in a hot mixture of ethanol (300 mL) and water (150 mL). After adjusting the pH of the mixture to 3 with HCl (aqueous), the solution of *N*-hexylphenothiazine aldehyde (8.36 g, 25.16 mmol) in ethanol (100 mL) was added slowly. The resulting solution was refluxed at 90 °C for 8 h. The residue was washed with water several times, which produced a yellow powder.



Scheme S1: Synthetic scheme for **C3PTZ**.

C3PTZ: Yield 6.76 g (75%), m.p. 250-252 °C, IR (ν cm⁻¹, in KBr): 3568, 3054, 2953, 2929, 2868, 1773, 1718, 1631, 1603, 1574, 1551, 1495, 1465, 1442, 1395, 1364, 1333, 1286, 1249, 1218, 1162, 1101, 1040. ¹H NMR (400 MHz, CDCl₃) δ 11.13 (s, 3H), 8.47 (s, 3H), 7.87 (d, J = 6.5 Hz, 3H), 7.34 (s, 3H), 7.17 (dd, J = 8.0, 6.2 Hz, 3H), 7.09 (dd, J = 7.4, 0.5 Hz, 3H), 6.93 (t, J = 7.6 Hz, 3H), 6.83 (d, J = 8.0 Hz, 3H), 6.74 (d, J = 8.5 Hz, 3H), 3.70 (br, 6H), 1.91 (br, 6H), 1.32 (br, 12H), 0.88 (t, J = 7.0 Hz, 9H). ¹³C NMR (101 MHz, CDCl₃) δ 149.9, 147.2, 147.1, 144.1, 128.3, 127.4, 127.3, 127.1, 126.9, 123.8, 122.8, 115.5, 115.2, 47.8, 29.1, 26.4, 22.4, 14.1. HR-MS for C₅₅H₆₀N₆S₃⁺, calc. 942.4128, found 942.4266.

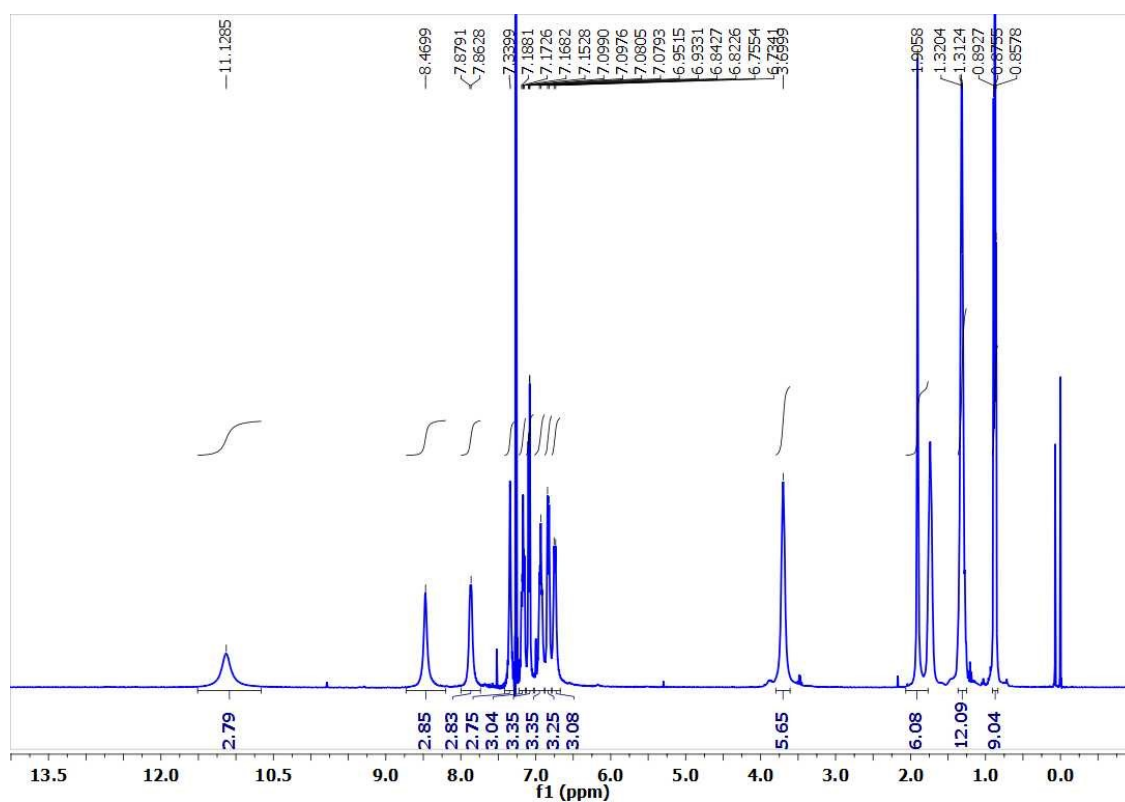


Figure S1: ¹H NMR spectrum of **C3PTZ** in CDCl₃.

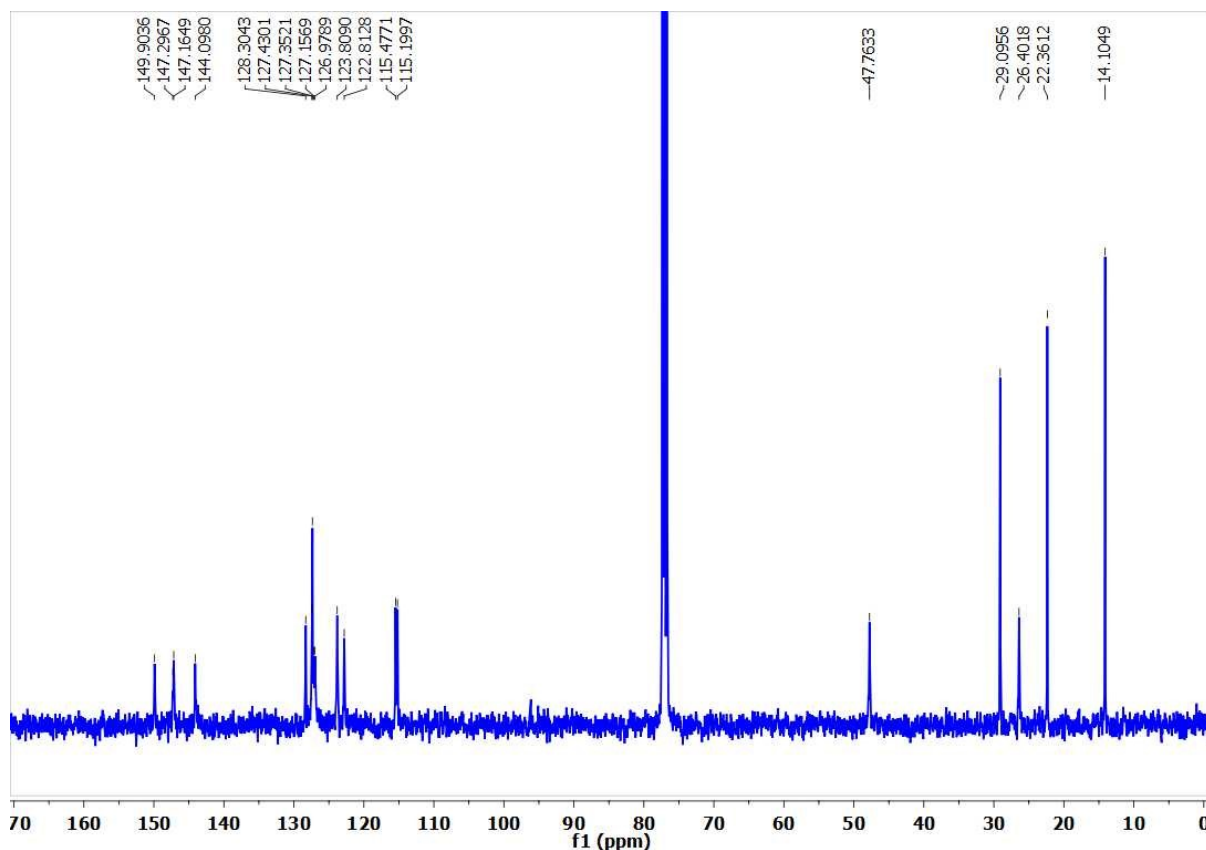


Figure S2: ^{13}C NMR spectrum of C3PTZ in CDCl_3 .

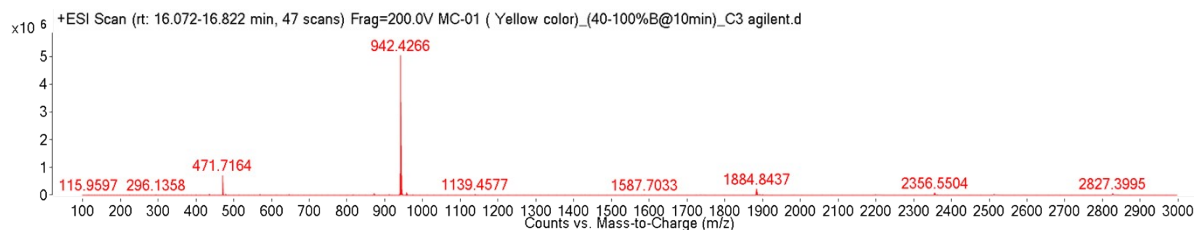


Figure S3: HR-MS spectrum for C3PTZ.

Methods and Measurements:

Steady-state absorption and fluorescence measurements: The electronic absorption spectra were recorded with a UV 3600 Plus (Shimadzu). The fluorescence spectra were recorded on a Hitachi spectrofluorometer (F7000, Japan) using a 1 cm pathlength quartz cuvette for solution-state spectra and Fluorolog, Horriba for solidstate emission spectra. A stock solution of 10^{-3} M was prepared in 1,4-dioxane. The final concentration of the probe was adjusted to $10\ \mu\text{M}$. The solid-state absorbance and emission spectra were recorded in the pristine, ground, thermal heating, solvent fumed solid samples.

Powder X-ray diffraction and IR spectra measurement: The powder X-ray diffraction (PXRD) pattern was recorded using a Rigaku Ultima IV X-ray diffractometer. The parameters were kept constant for the samples before and after the applications of stimuli: a step width of 0.2 with a scan rate of 21/min from 5-45° (Cu, Ka, $\lambda = 1.54\text{\AA}$). The IR spectra were recorded using an FTIR spectrometer (FT/IR-4200, Jasco). KBr was used as a matrix for recording the IR spectra.

Absolute quantum yield and lifetime decay measurement: The solid-state absolute quantum yield was measured using a calibrated integrating sphere method with an absolute error of 2%. Time-resolved fluorescence measurements were performed using a time-correlated single-photon counting (TCSPC) unit (Horiba Deltaflex). The laser used for all samples was 403 nm. Aluminum foil was used as the IRF for all of the solid samples. All measurements were performed at room temperature. The decay fitting was completed, keeping the χ^2 value close to unity.

Thermal analysis study: Thermogravimetric analysis (TGA) was carried out on a Shimadzu DTG-60 simultaneous DTATG apparatus with increasing temperature rate at 5 °C/min in N₂ atmosphere, and differential scanning calorimetry was recorded using a Themys One⁺ with a temperature range of 30-650 °C at 5 °C/min under N₂ atmosphere.

Computational Details:

Geometry optimizations of all the compounds are carried out with the aid of Density-Functional Theory (DFT) using B3LYP exchange-correlation functional and 6-31G(d) basis set, as implemented in the Gaussian 16 suite of programs.¹ Excited-states calculation were performed using time-dependent DFT (TD-DFT) methods with different DFT functionals (viz., B3LYP, PBE0, ω B97XD, M06-2X and LC- ω *PBE. ω value was tuned in LC- ω *PBE functional and found to be 0.154 Bohr^{2,3} From the TD-DFT calculation (Table S3), we found that LC- ω *PBE functional is the best choice for the optical properties of this molecule. The D3 version of Grimme's dispersion was included for dimer calculations.⁴ All of the DFT and TD-DFT calculations were done in acetonitrile ($\epsilon = 37.5$) using the polarizable continuum model (PCM).⁵ Long alkyl group attached with the N-atom (viz., -C₅H₁₁) of pentylphenothiazine

(PTZ), was substituted by methyl group to reduce the computational cost. Non-covalent interaction (NCI) plot calculations are carried out using Multiwfn 3.6 package.^{6,7}

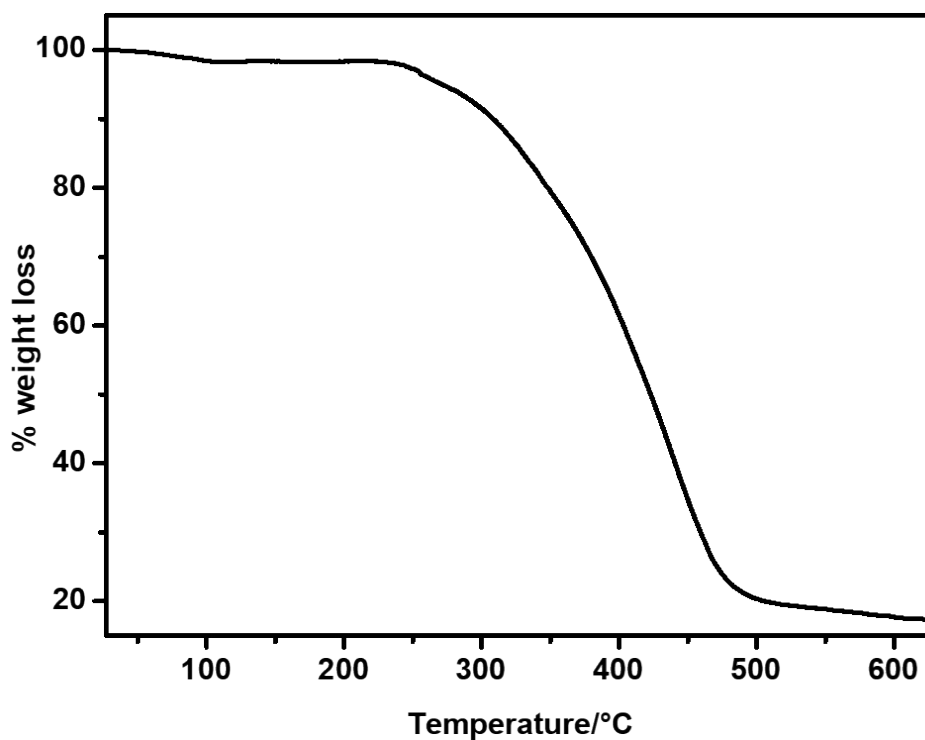


Figure S4: TGA plot for C3PTZ.

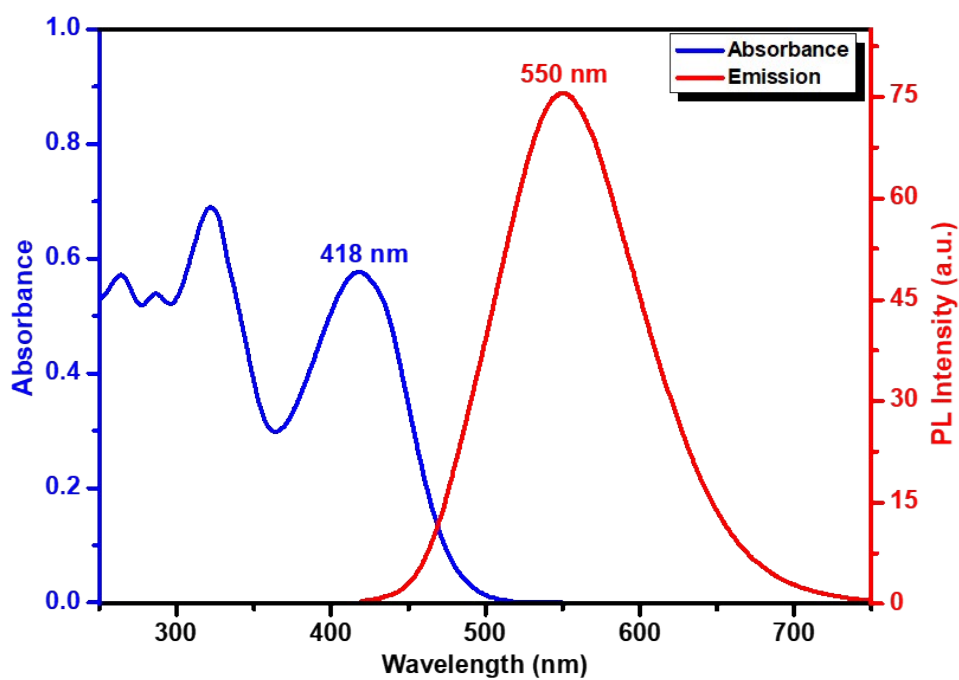


Figure S5: Absorption and FL spectra for C3PTZ, $\lambda_{\text{ex}} = 405$ nm.

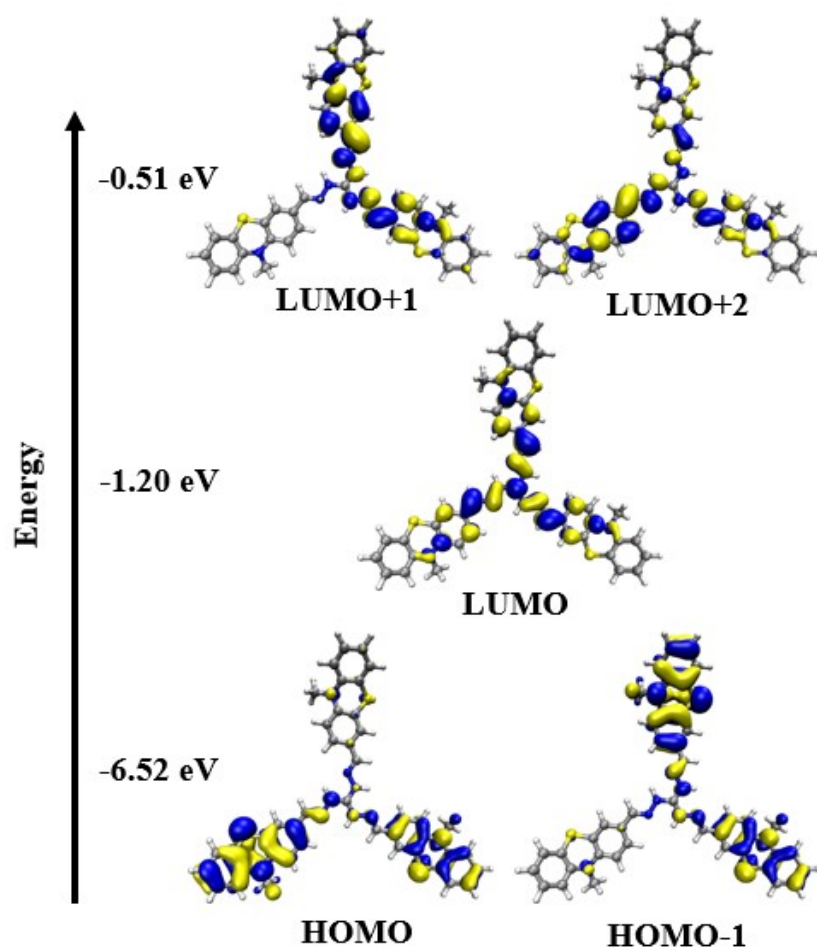


Figure S6: Frontier Molecular Orbitals (FMO)

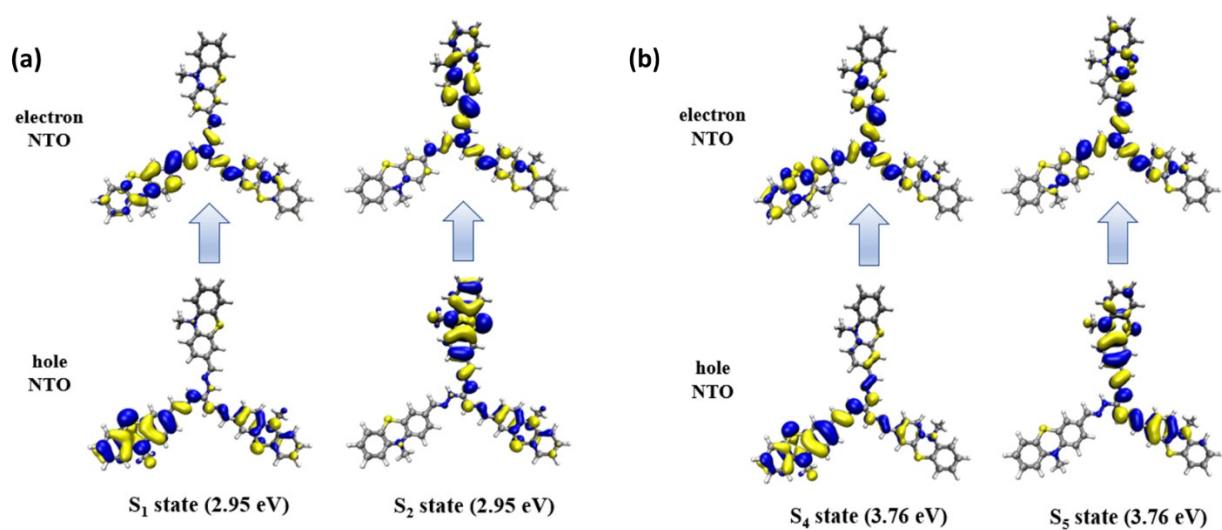


Figure S7: Natural transition orbitals (NTOs) for (a) S_1 and S_2 (b) S_4 and S_5 states.

Table S1: Calculated Lowest Energy (i.e., S_1 state) Optical Absorption using TDDFT (using Acetonitrile solvent)

DFT	B3LYP	PBE0	ω B97XD	M062X	LC- ω *PBE	Experiment
Energy (nm)	466	439	357	370	420	418
Oscillator strength	$f=0.61$	$f=0.71$	$f=1.08$	$f=0.97$	$f=0.91$	-

Table S2: Absorption Wavelength Excited States using LC- ω *PBE.

State	Calculated wavelength (nm)	Osc. Strength (f)	Configurations (H=HOMO, L=LUMO)	Expt. Absorption (nm)
S_1	420	0.91	H \rightarrow L (60%); [H-2] \rightarrow [L+2] (14%)	418
S_2	420	0.91	[H-1] \rightarrow L (60%); [H-2] \rightarrow [L+1] (14%)	418
S_3	394	0.00	[H-2] \rightarrow L (46%); [H-1] \rightarrow [L+1] (21%); H \rightarrow [L+2] (21%)	-
S_4	330	0.66	[H-6] \rightarrow L (9%); [H-3] \rightarrow L (17%); [H-2] \rightarrow [L+2] (10%)	326
S_5	330	0.66	[H-7] \rightarrow L (9%); [H-4] \rightarrow L (17%); H \rightarrow [L+1] (10%)	326

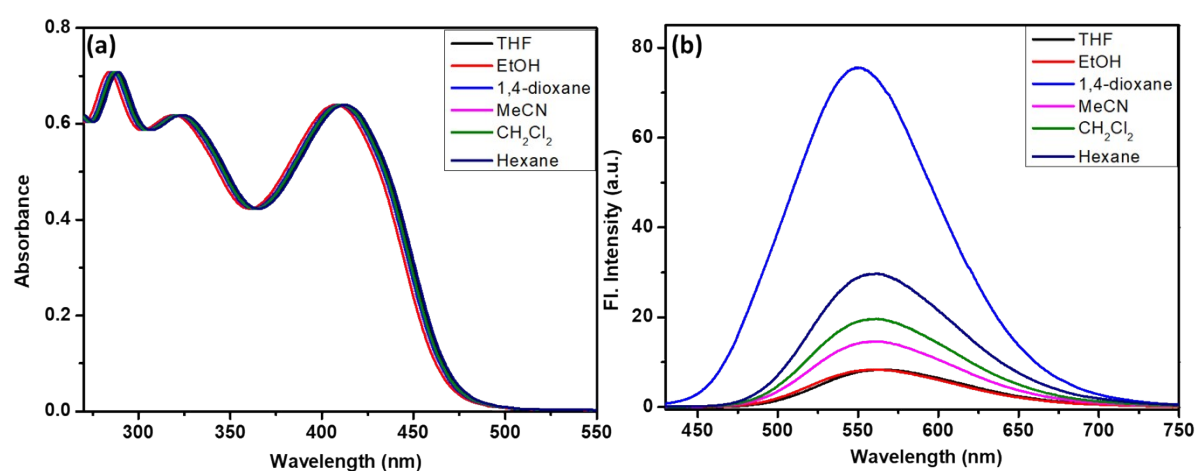


Figure S8: Absorption and FL spectra for C3PTZ in different solvents, $\lambda_{\text{exc}} = 405$ nm

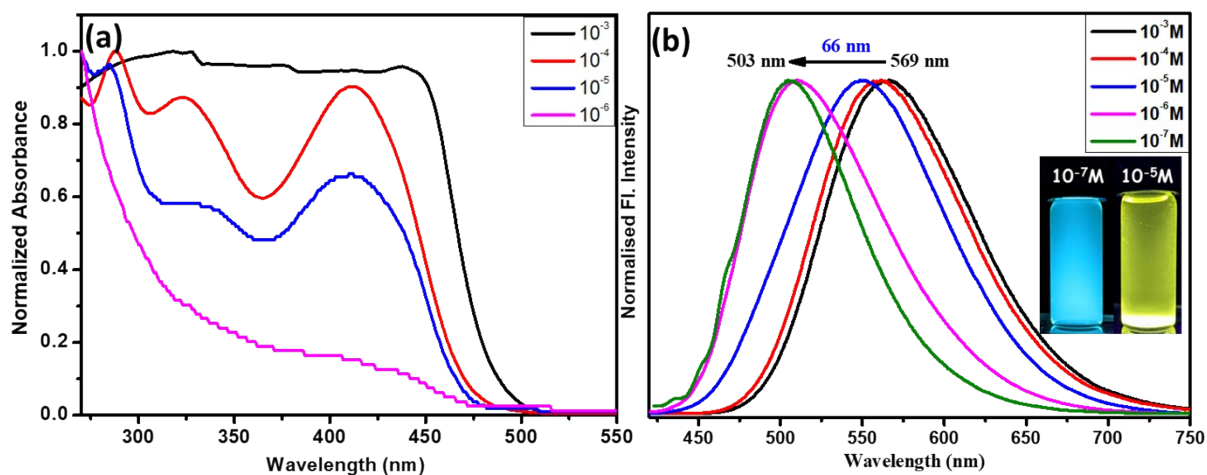


Figure S9: (a) Absorbance and (b) FL spectra for **C3PTZ** in 1,4-dioxane at different concentrations, $\lambda_{\text{ex}}=405$ nm.

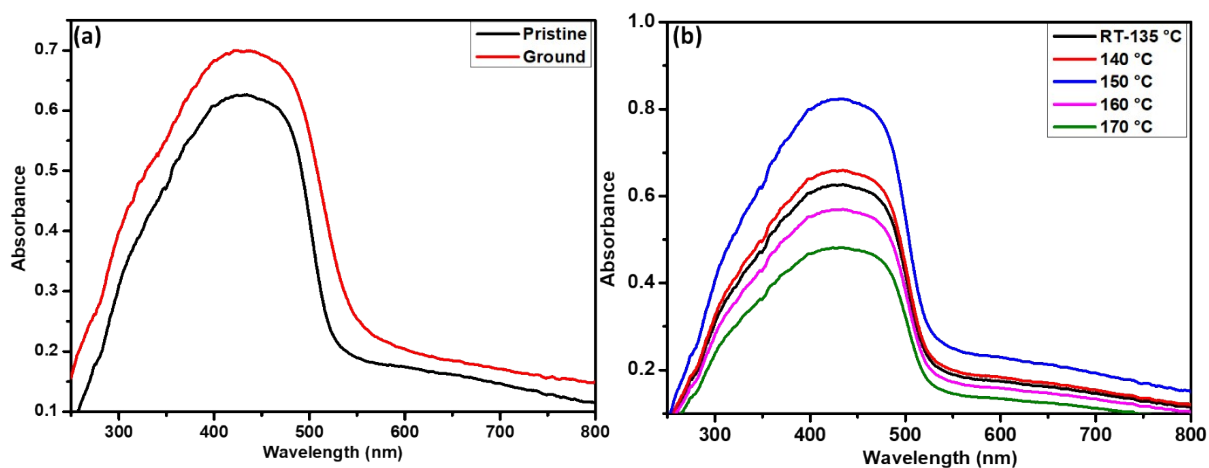


Figure S10: Absorption spectra for **C3PTZ** (a) before and after grinding and (b) at different temperatures.

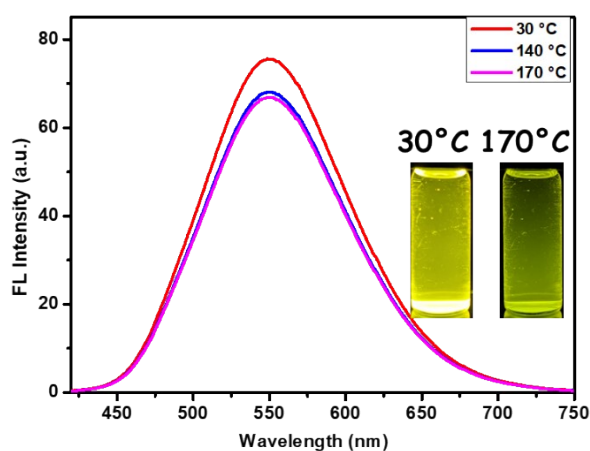


Figure S11: Temperature dependant FL spectra for **C3PTZ** in dimethyl acetamide.

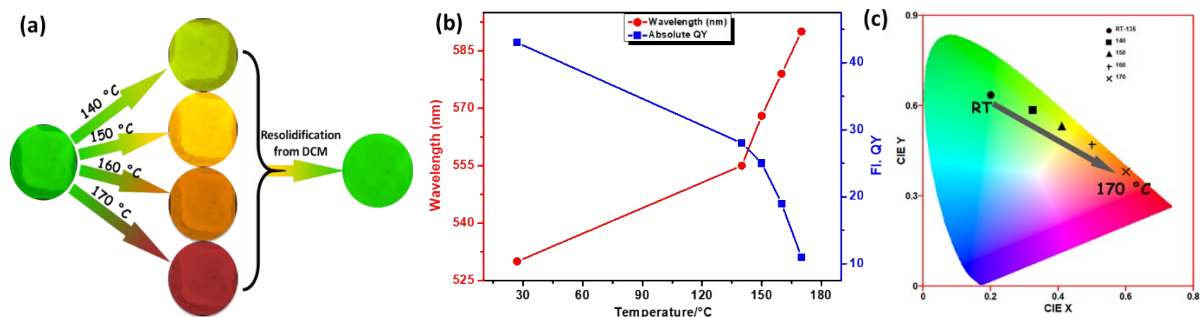


Figure S12: (a) Reversible thermochromic of C3PTZ upon resolidification from DCM. (under 365 nm UV lamp) (b) The plot of wavelength and absolute Φ_f vs. Temp (c) CIE chromaticity diagram with temp dependence.

Table S2: Photophysical parameters for C3PTZ

States	λ_{abs} (nm)	λ_{emi} (nm)	Φ_f (%)	CIE coordinate	$\langle\tau\rangle$ (ns)	K_r ($\times 10^6 \text{ s}^{-1}$)	K_{nr} ($\times 10^6 \text{ s}^{-1}$)	K_r/K_{nr}
Pristine	435	530	43	(0.210,0.630)	1.65	260.06	346.00	0.75
Ground	440	575	36		1.52	236.84	421.05	0.56
140 °C		555	28	(0.320,0.580)	1.37	204.38	525.55	0.38
150 °C		568	25	(0.412,0.530)	1.03	242.72	728.15	0.33
160 °C		579	19	(0.503,0.472)	0.87	218.39	931.03	0.23
170 °C		590	11	(0.604,0.380)	0.73	150.68	1219.18	0.12

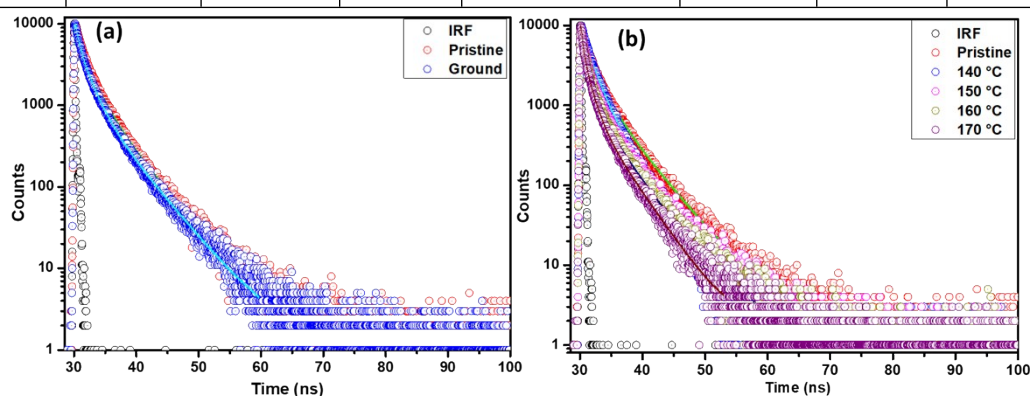


Figure S13: Lifetime decay plot for C3PTZ for pristine and after stimuli.

Table S3: Lifetime decay table for C3PTZ

States	τ_1 (ns)	τ_2 (ns)	τ_3 (ns)	α_1 (%)	α_2 (%)	α_3 (%)	χ^2	$\langle\tau\rangle$ (ns)
Pristine	1.78	0.43	4.63	0.43	0.42	0.15	1.10	1.65
Ground	1.46	0.38	3.32	0.47	0.32	0.21	1.09	1.52
140 °C	1.71	4.76	0.42	0.38	0.11	0.51	1.16	1.37
150 °C	1.36	0.30	4.35	0.35	0.56	0.09	1.10	1.03
160 °C	1.21	0.27	4.03	0.31	0.60	0.08	1.17	0.87
170 °C	1.14	3.78	0.26	0.28	0.06	0.66	1.23	0.73

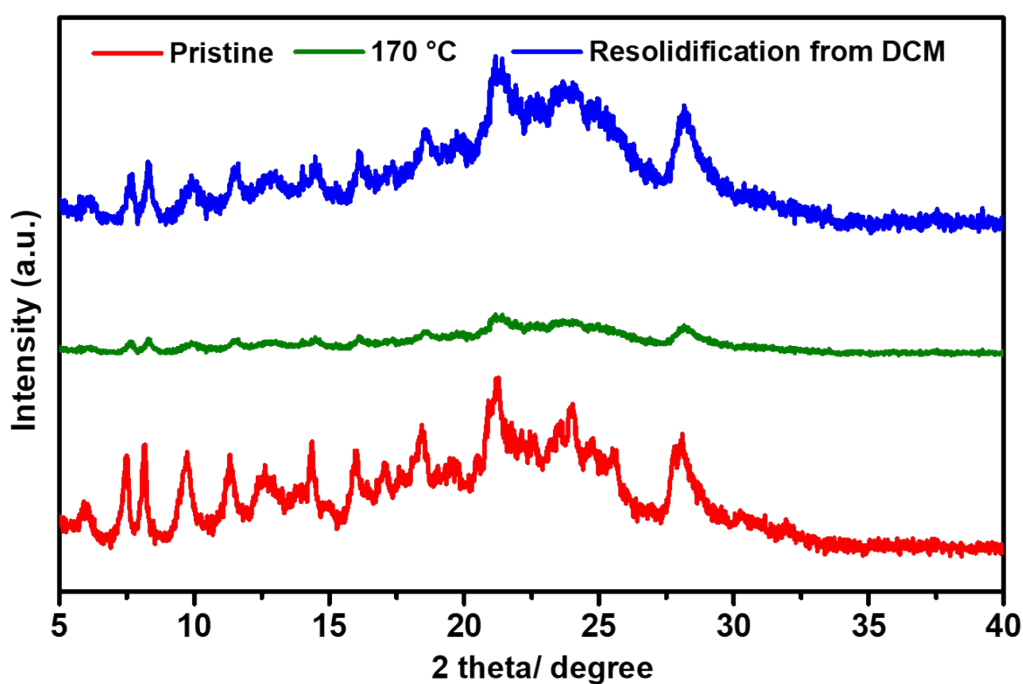


Figure S14: PXRD pattern for **C3PTZ** for pristine, 170 °C and resolidification from DCM.

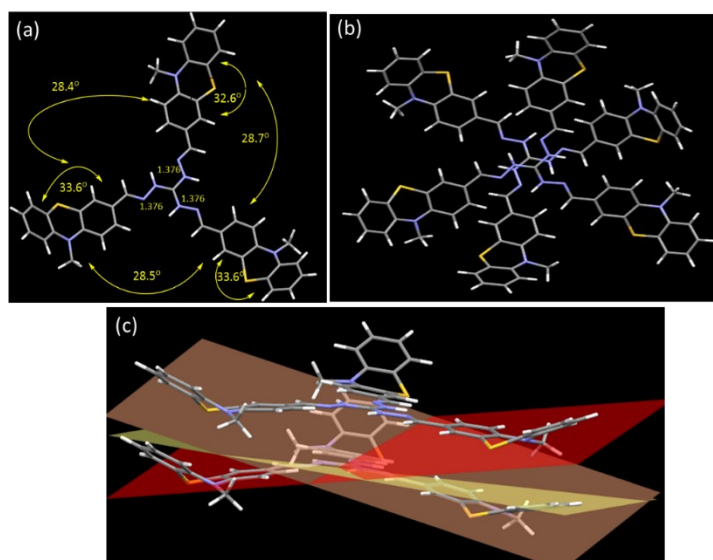


Figure S15: (a) Optimized molecular structure of **C3PTZ** with selected bond angles and distances. (b) staggered form (c) propeller-shape (shown in a molecule present in the dimer) with interplanar angles 12°, 15°, 23°.

Non-covalent Interaction (NCI) Calculation

The non-covalent interaction (NCI) method is used to study weak interaction. (Johnson *et al.*, J. Am. Chem. Soc. **2010**, *132*, 6498). In the Figure, the green colour iso surface between two molecules indicates weak $\pi \dots \pi$ interaction.

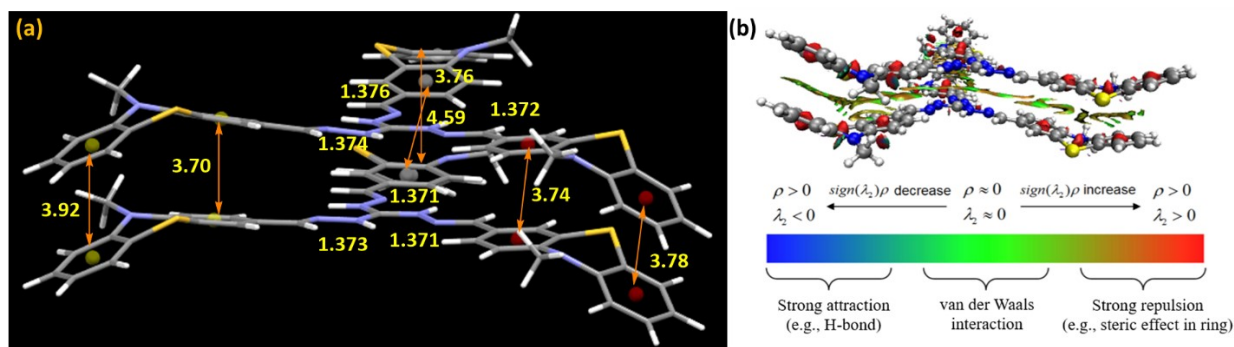


Figure S16: (a) Optimized **C3PTZ** dimer (eclipsed) with selected (N-N) bond lengths (Å) and possible centroid...centroid distances (Å). (b) Non-covalent interaction (NCI) plot with isovalue of 0.5 a.u. and λ_2 is the second largest eigenvalue of the Hessian matrix of electron density.

van der Waals interaction regions always have a very small value of electron density (ρ). On the other hand, the regions corresponding to strong steric effect or evident attractive weak interaction (e.g. H-bond, Halogen bond) have relatively large ρ value. However, the real-space

function sign $(\lambda_2)\rho$ is negative for attraction interaction and is positive for steric repulsion. λ_2 is the second largest eigenvalue of the Hessian matrix of electron density.

References:

1. Zhou, Y.; Li, Z. X.; Zang, S. Q.; Zhu, Y. Y.; Zhang, H. Y.; Hou, H. W.; Mak, T. C. W. A Novel Sensitive Turn-on Fluorescent Zn^{2+} Chemosensor Based on an Easy to Prepare C3-Symmetric Schiff-Base Derivative in 100% Aqueous Solution. *Org. Lett.* 2012, **14**, 1214-1217.
2. Gaussian 09, Revision E.01, M. J. Frisch, G. W. Trucks, H. B. Schlegel, G. E. Scuseria, M. A. Robb, J. R. Cheeseman, G. Scalmani, V. Barone, B. Mennucci, G. A. Petersson, H. Nakatsuji, M. Caricato, X. Li, H. P. Hratchian, A. F. Izmaylov, J. Bloino, G. Zheng, J. L. Sonnenberg, M. Hada, M. Ehara, K. Toyota, R. Fukuda, J. Hasegawa, M. Ishida, T. Nakajima, Y. Honda, O. Kitao, H. Nakai, T. Vreven, J. A. Montgomery, Jr., J. E. Peralta, F. Ogliaro, M. Bearpark, J. J. Heyd, E. Brothers, K. N. Kudin, V. N. Staroverov, T. Keith, R. Kobayashi, J. Normand, K. Raghavachari, A. Rendell, J. C. Burant, S. S. Iyengar, J. Tomasi, M. Cossi, N. Rega, J. M. Millam, M. Klene, J. E. Knox, J. B. Cross, V. Bakken, C. Adamo, J. Jaramillo, R. Gomperts, R. E. Stratmann, O. Yazyev, A. J. Austin, R. Cammi, C. Pomelli, J. W. Ochterski, R. L. Martin, K. Morokuma, V. G. Zakrzewski, G. A. Voth, P. Salvador, J. J. Dannenberg, S. Dapprich, A. D. Daniels, O. Farkas, J. B. Foresman, J. V. Ortiz, J. Cioslowski, and D. J. Fox, Gaussian, Inc., Wallingford CT, 2013.
3. H. Sun, C. Zhong and J. L. Bredas, *J. L.J. Chem. Theory Comput.* **2015**, *11*(8), 3851-3858.
4. S. Grimme, J. Antony, S. Ehrlich and H. Krieg, *J. Chem. Phys.* 2010, *132*, 154104–154123.
5. G. Scalmani and M. J. Frisch, *J. Chem. Phys.* **2010**, *132*, 144110.
6. E. R. Johnson, S. Keinan, P. Mori-Sánchez, J. Contreras-García, A. J. Cohen and W. Yang, *J. Am. Chem. Soc.* **2010**, *132*(18), 6498-6506.
7. T. Lu, F. Chen, *J. Comput. Chem.* **2012**, *33*, 580-592.

-----END-----